1-1-2018

CO2 electrolysis in seawater: calcification effect and a hybrid self-powered concept

Chong Yong Lee
University of Wollongong, cylee@uow.edu.au

Gordon G. Wallace
University of Wollongong, gwallace@uow.edu.au

CO2 electrolysis in seawater: calcification effect and a hybrid self-powered concept

Abstract

Oceans are regarded as a sink for anthropogenic CO2; as such seawater provides an attractive electrolyte for electrochemical CO2 reduction to value-added carbon-based fuels and chemical feedstocks. However, the composition of seawater is inherently complex, containing multiple cations and anions that may participate in the CO2 electroreduction reaction. Herein, examination of a nanoporous Ag electrocatalyst in seawater reveals a significant influence of calcium ions on the electrochemical CO2 reduction performance. Under the applied cathodic potential and in the presence of CO2, calcium ions in the seawater result in calcium carbonate deposition onto the nanoporous Ag, reducing active sites for CO2 electroreduction. Mitigation of calcification would promote a stable CO2 electrolysis in seawater. A first proof-of-concept self-powered hybrid CO2 electrolysis is demonstrated by the coupling of a Mg anode to a nanoporous Ag cathode in 0.6 M NaCl or seawater. A spontaneous oxidation of a Mg alloy at the anode drives cathodic reduction of AgCl to nanoporous Ag, which electrocatalytically reduces CO2 to CO. Combining galvanic and electrolytic properties in a single electrochemical cell offers a general approach for designing hybrid self-powered electrolysers. Strategies to overcome calcification such as removal of calcium from the seawater and development of anti-calcifying electrocatalysts are needed to promote practicability of seawater as an electrolyte in CO2 electroreduction technology.

Disciplines

Engineering | Physical Sciences and Mathematics

Publication Details

Lee, C. & Wallace, G. G. (2018). CO2 electrolysis in seawater: calcification effect and a hybrid self-powered concept. Journal of Materials Chemistry A, 6 (46), 23301-23307.

Journal Name

COMMUNICATION

CO_2 electrolysis in seawater: calcification effect and a hybrid self-powered concept

Received 00th January 20xx,
Accepted 00th January 20xx

DOI: 10.1039/x0xx00000x

www.rsc.org/

Chong-Yong Lee,*[a] and Gordon G Wallace*[a]

Oceans are regarded as a sink for anthropogenic CO_2, as such seawater provides an attractive electrolyte for electrochemical CO_2 reduction to value-added carbon-based fuels and chemical feedstocks. However, composition of seawater is inherently complex, containing multiple cations and anions that may participate in CO_2 electroreduction reaction. Herein, examination of a nanoporous Ag electrocatalyst in seawater reveals significant influence of calcium ions towards electrochemical CO_2 reduction performance. Under the applied cathodic potential and in the presence of CO_2, calcium ions in the seawater resulting in calcium carbonate deposition onto the nanoporous Ag, reducing active sites for CO_2 electroreduction. Mitigation from calcification would promote a stable CO_2 electrolysis in seawater. A first proof-of-concept self-powered hybrid CO_2 electrolysis is demonstrated by the coupling of a Mg anode to a nanoporous Ag cathode in 0.6 M NaCl or seawater. A spontaneous oxidation of a Mg alloy at anode driving cathodic reduction of AgCl to nanoporous Ag, which electrocatalytically reduces CO_2 to CO. Combining galvanic and electrolytic properties in a single electrochemical cell offers a general approach in designing hybrid self-powered electrolysers. Strategies to overcome calcification such as removal of calcium from the seawater, and development of anti-calcifying electrocatalyst are needed to promote practicability of seawater as an electrolyte in CO_2 electroreduction technology.

Introduction

As part of a CO_2 mitigation effort, the scientific community has long investigated a variety of approaches to capture and convert CO_2 to value-added products.[1-9] Electrochemical CO_2 reduction is one such attractive approach.[4-9] While enormous efforts have been devoted in developing highly efficient and selective CO_2 reduction electrocatalysts; examination on influence of the electrolytes has attracted growing interest. Dissolved ions in the electrolytes were reported affecting CO_2 electroreduction performance *via* parameters such as solution's bulk/localised pH and conductivity, specific adsorption on catalyst, and alteration in catalyst surface morphologies.[7-9]

Oceans currently absorb vast quantities of CO_2 released mainly by the burning of fossil fuels.[10-12] CO_2 dissolves into seawater where it reacts to initially form carbonic acid, before being converted in equilibrium to the hydrogen carbonate (HCO_3^-) and carbonate (CO_3^{2-}) ions. Having absorbed ~ 40 % anthropogenic CO_2 emissions, oceans acidity has increased by ~ 26 % since pre-industrial era, and this trend is expected to continue.[10-12] As such, seawater represents an extremely attractive electrolyte for CO_2 electroreduction: not only is it abundant, but its ability to serve as a sink for CO_2 and has an inherently high ionic conductivity. However, to date, seawater has been employed as an electrolyte for electrocatalytic water oxidation and proton reduction,[13-15]rarely for electroreduction of CO_2.

To the best our knowledge, the only reported use of seawater for electroreduction of CO_2 is from Nakata et. al.[16] They briefly used seawater as an electrolyte, and achieved a faradaic conversion efficiency of 36 % in formaldehyde formation using a boron doped diamond (BDD) electrode. However, no elucidation of factors affecting the poor CO_2 electroreduction performance was given, illustrating the complexity of such chemistry in the presence of the dissolved ions in seawater. Instead of an expensive BDD electrode; a cheaper, widely available and tunable nanostructured metallic based electrode with corrosion resistance feature would be desirable. We found that Ag/AgCl is an attractive choice. Ag/AgCl electrode is highly stable at wide range of chloride concentrations in electrochemical reference system. Interestingly, they served as a cathode material for water or seawater activated batteries;[17-19] this may also offer an opportunity to integrate battery-type galvanic feature to the intended CO_2 electroreduction process. More ever, halide-derived nanoporous Ag from AgCl is among the best performing Ag-based electrocatalysts,[20-27] exhibits outstanding performance with a high faradaic CO_2 to CO conversion efficiency at a low overpotential.[25-27]

[a] *ARC Centre of Excellence for Electromaterials Science, Intelligent Polymer Research Institute, AIIM, Innovation Campus, University of Wollongong, Wollongong, NSW 2500, Australia. Emails:* cylee@uow.edu.au; gwallace@uow.edu.au

†Electronic Supplementary Information (ESI) available. See DOI: 10.1039/x0xx00000x

Electrochemical CO_2 reduction is conventionally driven by the use of an external electricity.[4-9, 20-27] If the electricity could instead be readily generated internally within an electrochemical cell for CO_2 reduction, it offers an alternative simplified design of CO_2 electrolyser with dual-functionality in electrical power and carbon-based fuel generations. We demonstrate here such a concept by coupling of a spontaneous anodic magnesium oxidation reaction that produces H_2, whilst driving electroreduction of CO_2 to CO at the Ag-based cathode in saline water including seawater. Mg was selected for this proof-of-concept study as it is light-weight, environmental friendly, possesses high theoretical voltages, and has been employed as a standby power source in land, and also undersea power sources.[28] In this communication, we examined and compared the CO_2 electroreduction performance of nanoporous Ag in 3.5 wt % NaCl and seawater, and investigated the influence of dissolved ions presence in the seawater. We also discussed the features of our proof-of-concept self-powered hybrid system, and it broader range of implication.

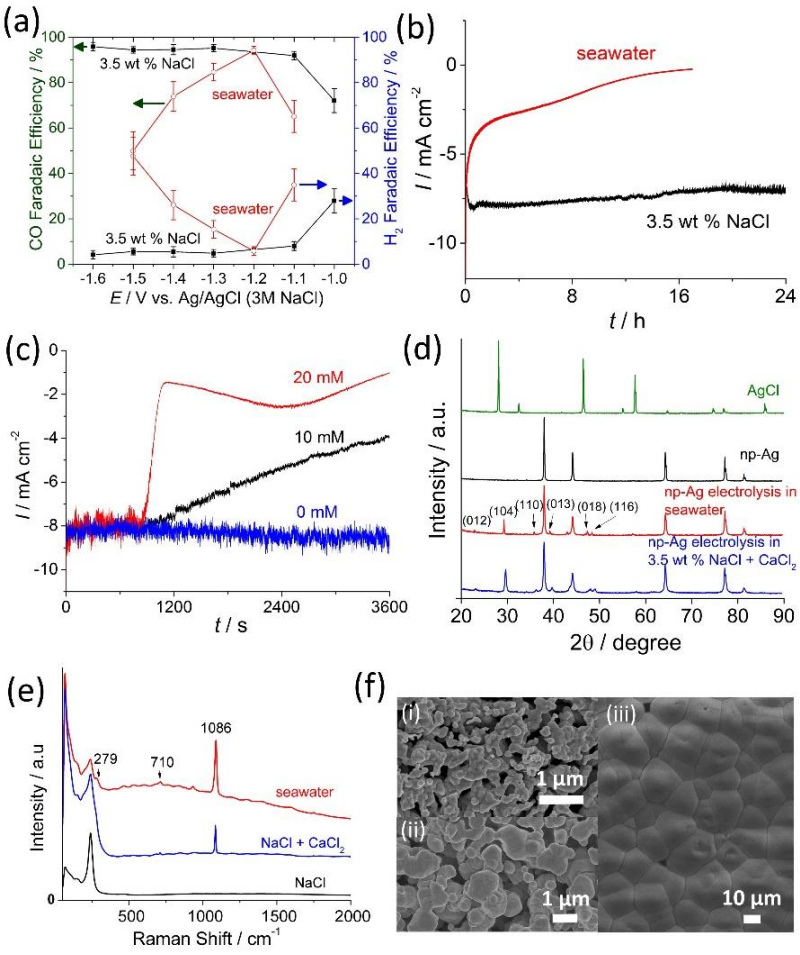

Figure 1 (a) Faradaic CO and H_2 conversion efficiencies as a function of applied potentials for CO_2 electroreduction performed on a nanoporous Ag in seawater and 3.5 wt % NaCl. (b) Current-time plot with long-term electrolysis of nanoporous Ag performed in seawater and 3.5 wt % NaCl at a fix potential of -1.40 V vs. Ag/AgCl (3M NaCl). (c) The effect of introducing 10 mM and 20 mM $CaCl_2$ to the 3.5 wt % NaCl electrolyte towards electrocatalytic CO_2 reduction at -1.40 V vs. Ag/AgCl (3M NaCl), $CaCl_2$ was injected at 900 s. (d) XRD patterns of the as formed Ag/AgCl; the nanoporus Ag (np-Ag) formed by electroreduction of AgCl; the np-Ag after undergone electrolysis in seawater and 3.5 wt % NaCl in the presence of 20 mM $CaCl_2$, respectively. (e) Raman spectroscopy of the corresponding electrodes as described in the XRD analysis. (f) SEM data of the (i) nanoporous Ag, (ii) nanoporous Ag after 24 h electrolysis in 3.5 wt % NaCl, and (iii) nanoporous Ag after 16 h electrolysis in seawater.

Results and discussion

Ag/AgCl electrodes employed in this work were prepared by a simple anodisation of Ag foils. Interplay of chloride concentrations and applied potentials not only allow rapid formation of Ag/AgCl layers, but tunable surface morphologies.[25] Considering the electrolytes for CO_2 electroreduction were with salinity of ~ 3.5 wt % NaCl, 0.6 M NaCl was employed as an electrolyte for the anodic formation of Ag/AgCl film. Figure S1 (ESI†) shows the representative SEM top and cross-sectional views of the Ag/AgCl electrode formed in 0.6 M NaCl solution, at 1.0 V for 300 s. A AgCl film of ~ 10 µm thick, with negligible nanosheets on the microstructure was obtained. Upon electrochemical reduction at -1.4 V (vs. Ag/AgCl (3M NaCl)) for 900s (Figure S2, ESI†) to convert AgCl to Ag, a halide-derived Ag with the nanoporous structures of around ~ 120 ± 50 nm (Figure 1f(i)) was formed.

We examine the performance of chloride-derived nanoporous Ag electrodes for cathodic CO_2 reduction process. Figure 1a shows the plot of CO_2 to CO conversion faradaic efficiency versus applied potential recorded under 1 h electrolysis in 3.5 wt % NaCl and seawater, respectively. In 3.5 wt % NaCl, CO_2 to CO conversion efficiencies were consistently above 90 % up to -1.1 V, and dropped to ~ 72 ± 5 % at -1.0 V vs Ag/AgCl (3M NaCl). In seawater, the conversion efficiency is strongly dependent on the applied potentials. The highest faradaic efficiency of ~ 93 ± 3 % was achieved at -1.2 V, but dropped to 65 ± 4 % at -1.1 V. Noted that the electrolysis at these two potentials were stable over 1 h electrolysis, but at -1.3 V and above, electrocatalytic currents in the first 10 min were unstable (Figure S3a, ESI†). Concurrently, the faradaic efficiencies also dropped to about 85, 70 and 50 % at -1.3 V, -1.4 V and -1.5 V, respectively. The higher cathodic potentials enhanced the localised pH change, which may promote the precipitation of calcium carbonate on the electrocatalytic sites of nanoporous Ag that subsequently influencing the faradaic conversion efficiencies. H_2 constitutes to the remaining percentage of the generated products in both NaCl and seawater electrolytes. No other gas or liquid phase product was detected.

We further examined the long-term stability of the reduced nanoporous Ag electrodes. Seawater as an electrolyte results in a much lower stability in comparison to the 3.5 wt % NaCl (Figure 1b). The electrocatalytic current drop significantly in the first few hours, and further drop to negligible current density. At -1.20 V (Figure S3b, ESI†), although a greater initial stability was achieved, but it also dropped substantially after the first 3 h. In contrast, a 24 h electrolysis at -1.40 V vs. Ag/AgCl (3M NaCl) in 3.5 wt % NaCl, an

excellent consistency in the catalytic current density is shown. The initial faradaic current efficiency for conversion of CO_2 to CO is found to be ~ 95 %, and dropped to ~ 79 % and ~ 75 % in 12 h and 24 h, respectively.

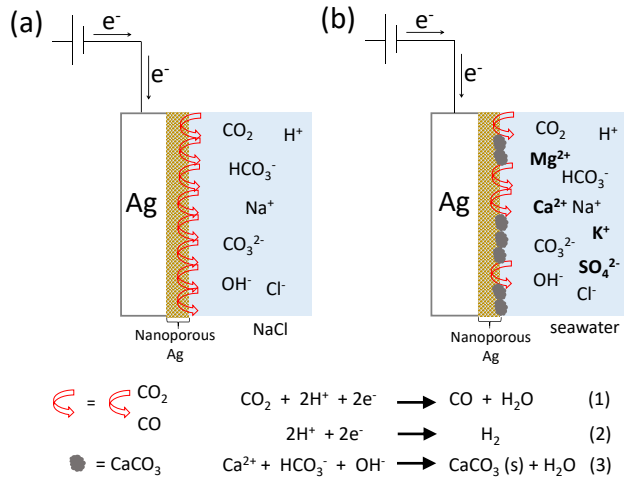

Figure 2 Schematic illustration of the interactions of dissolved ions in salt water (a) and seawater (b), under CO_2 purging and an applied cathodic potential. In NaCl electrolyte, the competition to CO_2 reduction (eq.1) is proton reduction reaction (eq. 2). The complexity of seawater as an electrolyte in the presence of several additional major ions is highlighted in bold (seawater also constitutes other ~ 0.7 % minor ions, which is not shown here). The applied cathodic potential induces localised pH change results in calcite precipitation on the nanoporous Ag (eq. 3). This reduces the available active sites of Ag to perform CO_2 electoreduction (represents by red arrows).

A typical seawater consists of major dissolved ions such as 55 % Cl^-, 30.6 % Na^+, 7.7 % SO_4^{2-}, 3.7 % Mg^{2+}, 1.2 % Ca^{2+} and 1.1 % K^+.[29] To elucidate the plausible reason for a lower stability and poorer performance of nanoporous Ag in the seawater, in addition to ~ 3.5 wt % Na^+, Cl^-; we introduced other seawater constituents SO_4^{2-}, Mg^{2+}, Ca^{2+} and K^+. The addition of SO_4^{2-}, Mg^{2+} and K^+ at 20 mM did not affect the electrocatalytic current, and the CO conversion faradaic efficiencies (Figure S4, ESI†). However, introduction of Ca^{2+} resulted in a detrimental effect towards electrocatalytic CO_2 reduction (Figure 1c). Increased concentration of the $CaCl_2$ in the electrolyte from 10 mM to 20 mM leads to a significant drop in the catalytic current.

XRD analysis in Figure 1d indicates the formation of calcite for both reduced Ag electrodes in seawater and 3.5 wt % NaCl solution intentionally added with 20 mM $CaCl_2$. The diffraction intensity of calcite at (104) was the strongest, with other peaks at (013), (116), (018), (110) and (012).[30] XRD data also indicates the expected reduction of AgCl to Ag upon the electro-reduction.[25] Raman analysis performed using a laser of 638 nm presented in Figure 1e shows the principal Raman shift of 1086 cm^{-1}, with weaker satellite peaks were observed with frequency shifts of 279 cm^{-1} and 710 cm^{-1}, all indicating signature peaks of calcite.[29] XPS analysis further confirms the formation of calcium calcite (Figure S5, ESI†). SEM images of Figure 1f shows structural change, with a larger particle size of nanoporous Ag obtained in 24 h (Figure 1f(ii)) in comparison to the electrolysis in 3.5 wt % NaCl for 1 h (Figure 1f(i)). In seawater, there was a significant deposition of calcite with patch sizes of ~ 10 to 20 µm on the electrode surface (Figure 1f(iii), Figure S6, ESI†).

Supported by the evident of calcite formation, we propose that Ca^{2+} containing seawater results in an electrochemically driven calcite precipitation onto nanoporous Ag (Figure 2, eq. 3). The localised increase of the pH resulting from CO_2 reduction at Ag active sites induces precipitation of calcite on the Ag catalyst. This is consistent with our pH measurement indicates decreased acidity of seawater as experiment progress. The type of substrate and hard water composition could significantly influence such electrochemical scaling process.[31-32] In this study, nanoporous Ag in contact with seawater preferentially deposited calcite, and this process is competing with CO_2 and H^+ reduction reactions (eq. 1 and 2). As such, the available Ag active sites for CO_2 electroreduction decreased gradually with the increment of deposit.

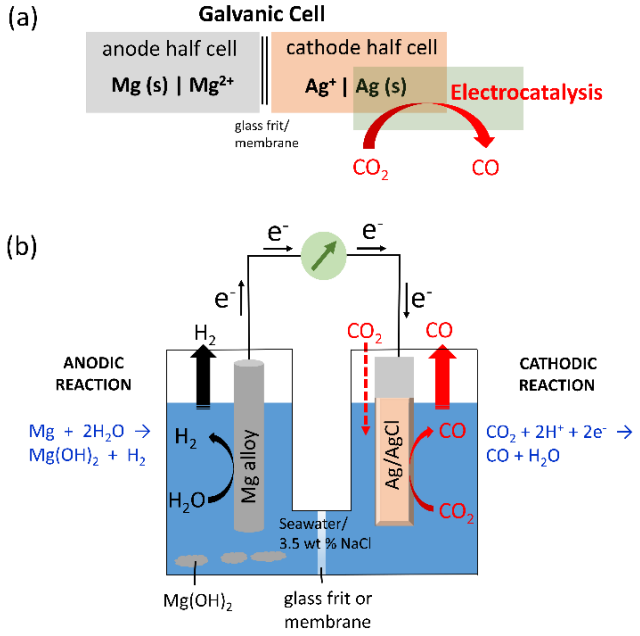

Figure 3 (a) Diagram of a galvanic cell consisting of a Mg as anodic half-cell that is oxidize to Mg^{2+}, and Ag^+ is reduce to Ag at the cathodic half-cell. An overlapping box to the cathodic half reaction represents an electrolytic process of catalytic conversion of CO_2 to CO by the reduced Ag. (b) Schematic diagram of the assembly of an electrochemical cell to generate H_2 and CO. Anodic and cathodic compartments were consisting of a Mg alloy and a Ag/AgCl electrodes, respectively.

Taking advantage of the feasibility of the CO_2 electroduction in saline water, we examine the possibility of driving cathodic reaction by coupling with an anodic process which could generate galvanic currents. Such a hybrid concept of a galvanic reaction driven an electrolytic process is illustrated in Figure 3. A galvanic cell is consisting of two half-cells connected by a membrane or a glass frit; a Mg and a Ag^+ (eg. AgCl in this work) serve as an anode and a cathode, respectively. A Mg anode in a salt containing electrolyte is spontaneously oxidise to Mg^{2+},[33-35] and the electrons resulting from the galvanic reaction flow to cathode for electroreduction of Ag^+ to Ag. In the presence of CO_2 as a reactant at the cathodic compartment, the reduced Ag acts as an electrocatalyst converts CO_2

to CO. This half-cell electrolytic reaction of CO_2 catalytic conversion is therefore powered by an internal galvanic cell.

Figure 4a illustrates the electrochemical behavior of the proposed cell-assembly *via* a combine plot from half-cell studies of cathodic CO_2 reduction and anodic Mg oxidation processes. Evidently, as an oxidation of Mg occurs at a more negative potential than cathodic CO_2 reduction process; spontaneously oxidative process is readily generating electricity within the assembled cell to drive the cathodic CO_2 reduction to CO by the nanoporous Ag. In contrast, a typical CO_2 reduction electrochemical device exhibits a more positive anodic potential than that the counterpart cathodic reaction, whereby the potential difference determines the external bias potential needed to drive the reaction.[36,37]

To examine the concept of a self-powered system; anode and cathode in a two-compartmented cell was wiring with crocodile clips, without loading any external electrical power supply (Figure S7, Video S1, ESI †). Our examination of an open circuit potential of the cell assembly in a two-compartment configuration show the value of ~ 1.58 V ± 0.04 with the used of Ag/AgCl electrode (Figure S8, ESI†). Upon the electrical connection, AgCl film was gradually reduced to nanoporous Ag as evidenced by a brownish AgCl changed to a silver-grey Ag. This conversion process to produce electrocatalytically active nanoporous Ag is typically completed around 20 minutes. This step was identical to the chronopotentiometry measurement (Figure S9, ESI†), but the electroreduction of AgCl instead was driven by electrons generated from the spontaneous oxidation of Mg. The galvanic current then proceed to drive the CO_2 electroreduction at the reduced nanoporous Ag. As illustrated in Figure 1b, H_2 and CO was generated simultaneously in the anodic and cathodic compartments, respectively.

We collected and quantified the H_2 and CO gases, with the plots of moles of generated H_2 and CO are shown in Figures 4b and 4c. As a result of oxidation of Mg alloy, H_2 was generated spontaneously and increased with time. Mg alloy in 3.5 wt % NaCl produced more H_2 in comparison to the seawater as anodic dissolution was faster in this medium. Consequently, CO production in seawater was lesser than that in 3.5 wt % NaCl. Although with a slower production rate as the experiment progress, CO was continually generated up to ~ 4 h in seawater which implies a slower rate of calcite deposition on the Ag surface in this self-powered assembly. Otherwise, a poorer stability of the nanoporous Ag with a quicker decay of CO production may occur, as was the case of half-cell study of CO_2 electroreduction at -1.4 V in seawater (Figure 2b). In additional to CO, a small amount of H_2 was also generated in the cathodic compartment (see Figure S10, ESI†), with no other product was detected. Control experiments with bare Ag foils in 3.5 wt % NaCl and seawater produce a very small quantity of CO (less than 1 µmol cm^{-2} after 5 h electrolysis), indicating the role of nanoporous Ag in activation of CO_2 electroreduction.

Comparison of SEM images of the Ag electrodes after 5 h electrolysis is shown in Figure 4d. A nanoporous feature was observed for the reduced Ag electrode performed in a NaCl electrolyte. However, in seawater, a larger feature sizes around 1 to 2 µm was observed that indicated the deposition of calcite onto the reduced nanoporous Ag. This is confirmed by detection of peaks corresponding to calcite from XRD and Raman data (Figure S11, ESI†). For the anodic part, XRD of Figure S12 (ESI†) confirmed the by-product from the oxidation of Mg producing $Mg(OH)_2$.

We show in this study the suitability of AgCl-derived nanoporous Ag to operate for CO_2 electroreduction to CO in saline electrolyte. The halide-derived electrocatalyst including AgCl has been reported offered an advantage of significantly suppress hydrogen evolution reaction.[25-27] The reaction mechanism is believed involving a multiple-step overall two-electron reduction of CO_2 to CO process as described in the previous studies.[20, 26] In salt water, high selectivity towards CO production (> 90 % conversion efficiency) was achieved, with the retention of faradaic efficiency of up to ~75 % over one day of electrolysis. CO conversion faradaic efficiency of ~ 90 % was achieved at -1.2 V vs Ag/AgCl (3M NaCl) in seawater, but with reduced long-term stability. The presence of calcium in seawater is found not only decreased the stability of the Ag catalyst; but also decreased the selectivity in CO conversion. To minimise the impact of Ca^{2+} in seawater in the direct electrochemical CO_2 conversion, existing technologies, such as ion exchange resins,[38,39] and precipitation agents[40] are readily available to remove Ca^{2+} from seawater before being employed as an electrolyte.

In our proof-of-concept demonstration of a self-powered hybrid system, we employed a magnesium alloy to serve as the anode. This serves two purposes: its direct reaction with saline water spontaneously generate H_2, producing $Mg(OH)_2$ that precipitates in the solution as the sole by-product; and its high activity drives a galvanic current that ultimately reduces CO_2. The rate limiting factor of the present system was the long-term stability of the halide-derived Ag catalyst in

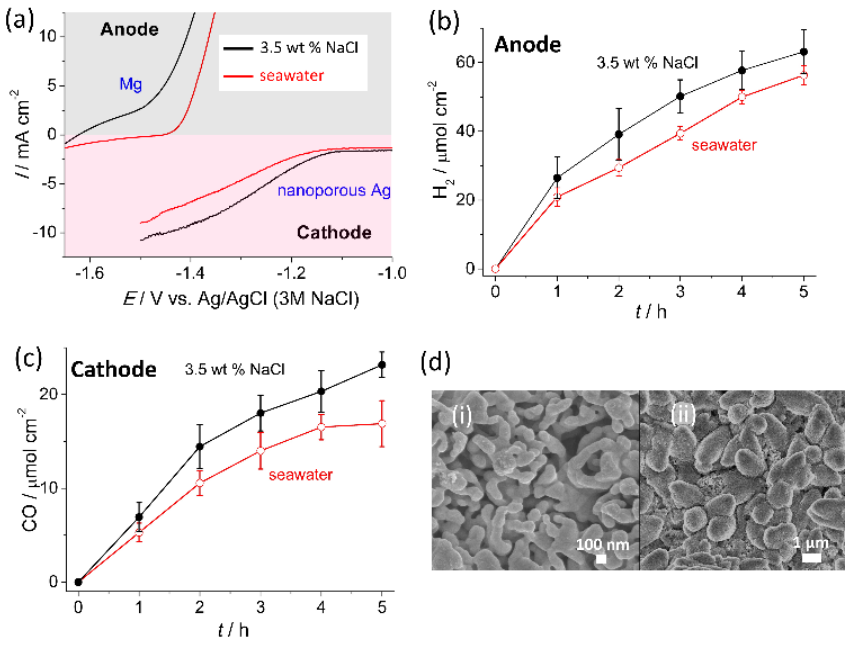

Figure 4 (a) The voltammograms recorded in a three-electrode configuration for anodic oxidation of a Mg alloy, and cathodic CO_2 reduction on a chloride-derived nanoporous Ag, in 3.5 wt % NaCl and seawater. Plots of moles of H_2 (b) and CO (c) obtained from the anodic and cathodic compartments, over 5 h self-powered full-cell assembly. (d) Representative SEM images of the Ag/AgCl samples after electroreduction in the self-powered full-cell assembly in 3.5 wt % NaCl (i) and seawater (ii).

performing CO_2 reduction, as excess of electrons were generated from the anodic dissolution of Mg. Mg in this demonstration is serving as a primary cell, where the spent Mg anode can be replaced, as is the case of Mg-based battery systems.[28]

Our proposed compartmented self-powered electrochemical cell facilitates the coupling of various anode and cathode materials, therefore it is important to emphasis that the self-powered concept demonstrated here is not limited to the use of Mg as an anode, or Ag/AgCl as a cathode. As Mg production is relatively energy-intensive, other sustainable anode materials that generating valuable anodic products would be desirable. Ag/AgCl employed as a cathode for CO_2 reduction in this work generates CO through two proton-coupled electron transfers. Other CO_2 reduction electrocatalyst materials that capable in generation of long chain (C_4-C_{12}) carbon products which consumed up to 12 electrons could be examined for in this hybrid system.[41,42]

As more efficient CO_2 reduction electrocatalysts to accommodate wide-ranging products are expected to be developed as the field progress; such a self-powered concept could serve to accommodate ad hoc and tasked-specific generation of desirable carbon-based products. For example, accessibility to electricity maybe limited in remote, undersea and military areas; this technology offers dual functionalities where the users could generate electricity and/or desirable carbon-based fuels. The required CO_2 could be integrated and sourced from the advanced materials that capable of releasing the stored CO_2.[1, 43] Hence, the proposed self-powered concept is intended to serve as a portable system for tasked-specific niche applications. This is a complimentary technology to the large-scale carbon-based fuel generation approach powered by an external renewable electricity, such as from solar and wind, with CO_2 obtained from the fossil fuel power plant. Importantly, recent advances in aqueous-based magnesium and other metallic secondary cell batteries,[28,44-46] offers a prospect to further advance such a self-powered concept to be rechargeable; where one could store the renewable electricity, and generating carbon-based fuels in a single aqueous-based electrochemical cell.

Conclusions

In summary, seawater is employable as an electrolyte for CO_2 electroreduction. Calcium ions in the seawater could be viewed as an undesirable interference species with respect to durability and efficiency of a CO_2 reduction electrocatalyst; in contrast, its high affinity for CO_2 means that it may serve as a useful species to electrochemically capture and store CO_2. A follow-up study will focus towards two key directions: finding an effective and simple strategy to remove calcium from the seawater, and developing anti-calcification coating on the electrocatalyst; with the aim of achieve a long-term stable and durable CO_2 electroreduction in seawater. The first proof-of-concept self-powered aqueous-based CO_2 electrolyser that we presented here is readily extendable to the rational coupling of other anodes and cathodes that could trigger both galvanic and targeted electrocatalytic reactions. Future work by the incorporation of an aqueous-based secondary battery feature would allow a rechargeable self-powered CO_2 electrolyser concept. Renewable electricity could be stored to power the electrolyser, hence advocating a sustainable system in electricity storage and renewable fuels generation within a single electrochemical cell.

Conflicts of interest

There are no conflicts to declare.

Acknowledgements

This work was supported by the University of Wollongong's Vice Chancellor Research Fellowship (to CYL). Funding from the Australian Research Council Centre of Excellence Scheme (CE 140100012) is gratefully acknowledged. The authors would also like to thank Australian National Fabrication Facility-Materials Node (ANFF) and UOW Electron Microscopy Centre for equipment use. We thank John Bullock (Bennington College) for his useful comments on this manuscript.

References

1. M. Aresta, A. Dibenedetto and A. Angelini, *Chem. Rev.,* 2014, **114**, 1709.
2. J. Artz, *Chem. Rev.,* 2018, **118**, 434.
3. D. P. Schrag, *Science,* 2007, **315**, 812.
4. J. H. Montoya, L. C. Seitz, P. Chakthranont, A. Vojvodic, T. Jaramillo and J. K. Nørskov, *Nat. Mater.,* 2017, **16**, 70.
5. C. W. Li and M. W. Kanan, *J. Am. Chem. Soc.,* 2012, **134**, 7231.
6. S. Gao, Y. Lin, X. Jiao, Y. Sun, Q. Luo, W. Zhang, D. Li, J. Yang and Y. Xie, *Nature*, 2016, **529**, 68.
7. C.-T. Dinh, T. Burdyny, Md. G. Kibria, A. Seifitokaldani, C. M. Gabardo, F. P. G. d. Arquer, A. Kiani, J. P. Edwards, P. D. Luna, O. S. Bushuyev, C. Zou, R. Quintero-Bermudez, Y. Pang, D. Sinton and E. H. Sargent, *Science,* 2018, **360**, 783.
8. S. Verma, X. Lu, S. Ma, R. I. Masel and P. J. A. Kenis, *Phys. Chem. Chem. Phys.,* 2016, **18**, 7075.
9. M. R. Singh, Y. Kwon, Y. Lum, J. W. Ager and A. T. Bell, *J. Am. Chem. Soc.,* 2016, **138**, 13006.
10. S. Khatiwala, T. Tanhua, S. M. Fletcher, M. Gerber, S. C. Doney, H. D. Graven, N. Gruber, G. A. McKinley, A. Murata, A. F. Rios and C. L. Sabine, *Biogeosciences*, 2013, **10**, 2169.
11. T. Devries, M. Holzer and F. Primeau, *Nature,* 2017, **542**, 215.
12. K. Caldeira and M. E. Wickett, *Nature,* 2003, **425**, 365.
13. S. Fukuzumi, Y.-M. Lee and W. Nam, *ChemSusChem,* 2017, **10**, 4264.
14. F. Dionigi, T. Reier, Z. Pawolek, M. Gliech and P. Strasser, *ChemSusChem,* 2016, **9**, 962.
15. N. Jiang and H.-M. Meng, *Surf. Coat. Techn.,* 2012, **206**, 4362.
16. K. Nakata, T. Ozaki, C. Terashima, A. Fujishima and Y. Einaga, *Angew. Chem. Int. Ed.*, 2014, **53**, 871.
17. I. C. Blake, *J. Electrochem. Soc.,* 1952, **99**, 202c.
18. J. B. Mullen and P. L. Howard, *J. Electrochem. Soc.* 1946, **90**, 520.
19. K. V. Rao, *Def. Sci. J.*, 2001, **51**, 161.
20. Y. Hori, in *Modern Aspects of Electrochemistry*, Volume 42 (Eds.: C. G. Vayenas, R. E. White; M. E. Gamboa-Aldeco), Springer New York, New York, USA, 2008, Ch. 3
21. Q. Lu, J. Rosen, Y. Zhou, G. S. Hutchings, Y. C. Kimmel, J. G. Chen and F. Jiao, *Nat. Commun.,* 2014, **5**, 3242.
22. L. Q. Zhou, C. Ling, M. Jones and H. Jia. *Chem. Commun.,* 2015, **51**, 17704.
23. C. Kim, H. S. Jeon, T. Eom, M. S. Jee, H. Kim, C. M. Friend, B. K. Min and Y. J. Hwang, *J. Am. Chem. Soc.,* 2015, **137**, 13844.
24. M. Ma, B. J. Trześniewski, J. Xie and W. A. Smith, *Angew. Chem. Int. Ed.,* 2016, **128**, 9900.
25. C.-Y. Lee, Y. Zhao, C. Wang, D. G. Mitchell and G. G. Wallace, *Sustainable Energy Fuels,* 2017, **1**, 1023.
26. Y.-C. Hsieh, S. D. Senanayake, Y. Zhang, W. Xu and D. E. Polyansky, *ACS Catal.,* 2015, **5**, 5349.

27. L. Zhang, Z. Wang, N. Mehio, X. Jin and S. Dai, *ChemSusChem,* 2016, **9**, 428.
28. T. Zhang, Z. Tao and J. Chen, *Mater. Horizons*, 2014, **2**, 149.
29. M. E. Q. Pilson, (1998). An introduction to the chemistry of the sea*, Prentice Hall,* N. J.
30. C. G. Kontoyannis and N. V. Vagenas, *Analyst*, 2000, **125**, 251.
31. C. Gabrielli, R. Jaouhari, S. Joiret, G. Maurin and P. Rousseau, *J. Electrochem. Soc.,* 2003, **150**, C478.
32. R. Jaouhari, A. Benbachir, A. Guenbour, C. Gabrielle, J. Garcia-Jareno and G. Maurin, *J. Electrochem. Soc.,* 2000, **147**, 2151.
33. A. Pardo, M. C. Merino, A. E. Coy, R. Arrabal, F. Viejo and E. Matykina. *Corros. Sci.,* 2008, **50**, 823.
34. N. Birbilis, M. K. Cavanaugh, A. D. Sudholz, S. M. Zhu, M. A. Easton and A. Gibson. *Corros. Sci.,* 2011, **53**, 168.
35. Z. X. Qiao, Z. M. Shi, N. Hort, N. I. Z. Abidin and A. Atrens, *Corros. Sci.,* 2012, **61**, 185.
36. D. A. Vermass and W. A. Smith, *ACS Energy Lett.,* 2016, **1**, 1143.
37. Y. C. Li, D. Zhou, Z. Yan, R. H. Goncalves, D. A. Salvatore, C. Berlinguette and T. E. Mallouck, *ACS Energy Lett.,* 2016, **1**, 1149.
38. H. R. Flodman and B. I. Dvorak, *Water Environ. Res.,* 2012, **84**, 535.
39. D. Clifford, T. J. Sorg and G. L. Ghurye, Ion exchange and adsorption of inorganic contaminants, in: J. K. Edzwald (Ed.) Water Quality & Treatment: A Handbook on Drinking Water, McGraw-Hill Inc., New York, NY, 2011.
40. R. I. Jeldres, M. P. Arancibia-Bravo, A. Reyes, C. E. Aguirre, L. Cortes and L. A. Cisternas, *Miner. Eng.*, 2017, **109**, 10.
41. B. Khezri, A. C. Fisher and M. Pumera, *J. Mater. Chem. A.,* 2017, **5**, 8230.
42. O. S. Bushuyev, P. D. Luna, C. T. Dinh, L. Tao, G. Saur, J. v. d. Lagemaat, S. O. Kelly and E. H. Sargent, *Joule,* 2018, **2***,* 825.
43. M. E. Boot-Handford, J. C. Abanades, E. J. Anthony, M. J. Blunt, S. Brandani, N. Mac Dowell, J. R. Fern´andez, M.-C. Ferrari, R. Gross, J. P. Hallett, R. S. Haszeldine, P. Heptonstall, A. Lyngfelt, Z. Makuch, E. Mangano, R. T. J. Porter, M. Pourkashanian, G. T. Rochelle, N. Shah, J. G. Yao and P. S. Fennell, *Energy Environ. Sci.* 2014, **7**, 130.
44. F. Wang, X. Fan, T. Gao, W. Sun, Z. Ma, C. Yang, F. Han, K. Xu and C. Wang, *ACS Cent. Sci.* 2017, **3**, 1121.
45. W. Ma, X. Liu, C. Li, H. Yin, W. Xi, R, Liu, G. He, X. Zhao, J. Luo and Y. Ding, *Adv. Mater.* 2018, **30**, 1801152.
46. J. Liu, C. Xu, Z. Chen, S. Ni and Z. X. Shen, *Green Energy & Environ.* 2018, **3**, 20-41.

